Am J Physiol Renal Physiol 318: F835–F842, 2020.
First published February 18, 2020; doi:10.1152/ajprenal.00505.2019.

RESEARCH ARTICLE

Exploring the role of the metabolite-sensing receptor GPR109a in diabetic nephropathy

Matthew Snelson,[1] Sih Min Tan,[1] Gavin C. Higgins,[1] Runa S. J. Lindblom,[1] and Melinda T. Coughlan[1,2]

[1]*Department of Diabetes, Central Clinical School, Alfred Medical Research and Education Precinct, Monash University, Melbourne, Victoria, Australia; and* [2]*Baker Heart and Diabetes Institute, Melbourne, Victoria, Australia*

Submitted 29 October 2019; accepted in final form 4 February 2020

Snelson M, Tan SM, Higgins GC, Lindblom RSJ, Coughlan MT. Exploring the role of the metabolite-sensing receptor GPR109a in diabetic nephropathy. *Am J Physiol Renal Physiol* 318: F835–F842, 2020. First published February 18, 2020; doi:10.1152/ajprenal.00505.2019.—Alterations in gut homeostasis may contribute to the progression of diabetic nephropathy. There has been recent attention on the renoprotective effects of metabolite-sensing receptors in chronic renal injury, including the G protein-coupled receptor (GPR)109a, which ligates the short-chain fatty acid butyrate. However, the role of GPR109a in the development of diabetic nephropathy, a milieu of diminished microbiome-derived metabolites, has not yet been determined. The present study aimed to assess the effects of insufficient GPR109a signaling, via genetic deletion of GPR109a, on the development of renal injury in diabetic nephropathy. *Gpr109a*$^{-/-}$ mice or their wild-type littermates (*Gpr109a*$^{+/+}$) were rendered diabetic with streptozotocin. Mice received a control diet or an isocaloric high-fiber diet (12.5% resistant starch) for 24 wk, and gastrointestinal permeability and renal injury were determined. Diabetes was associated with increased albuminuria, glomerulosclerosis, and inflammation. In comparison, *Gpr109a*$^{-/-}$ mice with diabetes did not show an altered renal phenotype. Resistant starch supplementation did not afford protection from renal injury in diabetic nephropathy. While diabetes was associated with alterations in intestinal morphology, intestinal permeability assessed in vivo using the FITC-dextran test was unaltered. GPR109a deletion did not worsen gastrointestinal permeability. Furthermore, 12.5% resistant starch supplementation, at physiological concentrations, had no effect on intestinal permeability or morphology. The results of this study indicate that GPR109a does not play a critical role in intestinal homeostasis in a model of type 1 diabetes or in the development of diabetic nephropathy.

diabetic nephropathy; dietary fiber; G protein-coupled receptor 109a; intestinal permeability; resistant starch

INTRODUCTION

Diabetic nephropathy is a major microvascular complication of diabetes, occurring in up to 30% of patients with type 1 diabetes (1). Concomitant with the rise in diabetes and obesity, the prevalence of diabetic nephropathy has been increasing rapidly, with diabetic nephropathy now the leading cause of end-stage renal disease worldwide (1). Despite optimal conventional management with pharmacological inhibition of the renin-angiotensin system and glycemic and blood pressure control, a significant proportion of patients with diabetic kidney disease still progress over time to end-stage renal failure. Thus, there is an urgent need for the identification of new therapeutic options to help limit the progression of this disease.

Recently, there has been an increasing interest in the diet-gut-kidney axis, whereby elements derived from the diet alter the composition of the gut microbiota and production of microbial metabolites, which induce effects at extraintestinal sites, including the kidneys (7, 8). It has been noted that patients with diabetes (10) and end-stage renal disease (11, 23) have a contraction in the bacterial taxa that produce beneficial short-chain fatty acids (SCFAs). Furthermore, during end-stage renal disease, there is an increase in intestinal permeability and subsequent inflammation (17). SCFAs act via local metabolite-sensing receptors to reduce intestinal permeability and inflammation (5, 9). The use of dietary therapies that directly target the gut microbiota to increase SCFA production, including probiotics and prebiotics, have been recently considered as potential adjunct interventions to limit injury in diabetic nephropathy (19).

Butyrate acts as a ligand for G protein-coupled receptor (GPR)109a, decreasing intestinal inflammation and promoting gut epithelial barrier integrity; thus, GPR109a activation is considered to be protective (16). A recent study (8) has shown that GPR109a modulated the renoprotective effect of butyrate on adriamycin-induced nephropathy; however, the role of GPR109a in the development of diabetic nephropathy has not been determined.

The present study aimed to assess the effects of insufficient GPR109a signaling via genetic deletion of GPR109a on the development of renal injury in diabetic nephropathy. *Gpr109a*$^{-/-}$ mice or their wild-type littermates (*Gpr109a*$^{+/+}$) were rendered diabetic with streptozotocin (STZ). Mice received a control diet or an isocaloric high-fiber diet containing 12.5% resistant starch (RS) for 24 wk, and gastrointestinal permeability and renal injury were determined.

MATERIALS AND METHODS

Animals. Male mice homozygous for deletion of the GPR109a receptor (*Gpr109a*$^{-/-}$) were obtained from Prof. Charles Mackay (Monash University, Melbourne, VIC, Australia) (16) and were crossbred with wild-type (WT) C57BL6/J mice purchased from the Jackson Laboratory to produce heterozygous mice, which were then mated to produce *Gpr109a*$^{-/-}$ knockout mice and WT littermate controls. Mice were housed in a climate-controlled animal facility that had a fixed 12:12-h light-dark cycle and were provided with ad libitum access to water and chow. All study protocols were conducted in accordance to the principles and guidelines devised by the Alfred Medical Research & Education Precinct Animal Ethics Committee

Address for correspondence: M. Snelson, Level 5, Alfred Centre, 99 Commercial Rd., Melbourne 3004, VIC, Australia (e-mail: matthew.snelson@monash.edu).

  ISSN 1931-857X.

(AMREP AEC) under the guidelines laid down by the National Health and Medical Research Council of Australia and had been approved by the AMREP AEC (E1487/2014/B).

Induction of diabetes. Diabetes was induced at 6 wk of age by five daily intraperitoneal injections of STZ (55 mg/kg ip, Sigma-Aldrich, St. Louis, MO) in sodium citrate buffer. Diabetes was confirmed by glycated hemoglobin (GHb) > 8%. Two mice failed to meet this cutoff and were excluded from any further analysis. Of those diabetic mice that were included in the analysis, the mean GHb was 11.7% (median: 11.9%).

Diet intervention. Since previous studies exploring the role of RS on the development of renal injury have used supraphysiological doses over a short period of time, we sought to supplement a dose of RS that could be more reasonably expected to be consumed by people [25% high-amylose maize starch (HAMS) Hi-maize 1043, equivalent to 12.5% RS] over a longer timeframe (24 wk). From 6 wk of age, mice received either a custom-made control diet or a high-fiber diet supplemented with RS prepared by Specialty Feeds (Perth, WA, Australia). Both of these semipure diets were formulated on the basis of a modified AIN93G growth diet for rodents. These diets were isocaloric, had equivalent protein, provided as 20% g/g casein, and fat, provided as 7% g/g canola oil. Each diet contained 5% g/g sucrose, 13.2% g/g dextrinized starch, and 7.4% g/g cellulose. A RS-supplemented diet (SF15-015) was formulated with 25% g/g Hi-maize 1043, whereas the control diet (SF15-021) contained an additional 20% g/g regular starch and 5% g/g cellulose to maintain caloric equivalency between diets. Hi-maize 1043, an RS2 starch prepared from HAMS, which contains 50% RS (15), was provided as a raw ingredient by Ingredion (Westchester, IL). Mice received these experimental diets ad libitum for 24 wk.

Tissue collection. At the end of the study period, mice were anesthetized by an intraperitoneal injection of 100 mg/kg body wt pentobarbital sodium (Euthatal, Sigma-Aldrich, Castle Hill, NSW, Australia) followed by cardiac exsanguination. Blood was immediately centrifuged at 6,000 rpm for 6 min, and plasma was snap frozen on dry ice and stored at −80°C. Kidney sections were fixed in neutral buffered formalin [10% (vol/vol)]. The gastrointestinal tract was dissected, and the mesentery was removed. Sections of the gastrointestinal tract were weighed, and length was measured. The ileum was flushed with chilled PBS. Ileum sections were fixed in paraformaldehyde [4% (vol/vol)] for 24 h before being transferred to 4% sucrose solution and embedded in paraffin. Ileum sections and renal cortical sections were snap frozen in liquid nitrogen and stored at −80°C.

Glycated hemoglobin. GHb was measured in blood collected at cull using a Cobas b 101 POC system (Roche Diagnostics, Forrenstrasse, Switzerland) according to the manufacturer's instructions. The Cobas b 101 POC system has a detection range of between 4% and 14%, with any sample with a GHb of <4% designated as low and samples with a GHb of >14% designated as high.

In vivo intestinal permeability assay. Intestinal permeability was assessed in vivo using the previously described dextran-FITC technique (4) during the week before cull. In brief, mice were fasted for a minimum of 4 h and received an oral gavage of a 125 mg/mL solution of dextran-FITC equivalent to 500 mg/kg body wt. After 1 h, ~120 μL of blood were collected from the tail vein using heparinized capillary tubes. Blood was centrifuged at 6,000 rpm for 6 min, plasma was collected, and the fluorescence in plasma samples was determined in relation to a standard dilution set using a fluorescence spectrophotometer (BMG Labtech, Ortenberg, Germany) set to excitation at 490 nm and emission at 520 nm. The intra-assay and interassay coefficients of variation were 3.2% and 8.9%, respectively.

Body composition. Fat mass and lean body mass were determined using a 4-in-1 EchoMRI body composition analyzer (Columbus Instruments, Columbus, OH), which measures fat mass, lean mass, and total water content using nuclear magnetic resonance relaxometry (14). The weight of mice before being placed in the body composition analyzer was used for the calculation of percent fat and lean mass.

Metabolic caging, urine, and plasma analyses. After 23 wk of experimental diet, mice were housed individually in metabolic cages (Iffa Credo, L'Arbresle, France) for 24 h for urine collection and measurement of urine output and food and water intake. Animals received ad libitum access to food and water during this period. Urine was stored at −80°C until required for analyses. Urinary albumin was determined using a mouse-specific ELISA (Bethyl Laboratories, Montgomery, TX) according to the kit protocol. The intra-assay and interassay coefficients of variation were 7.3% and 8.9%, respectively. Urinary monocyte chemoattractant protein-1 (MCP-1) was measured using a commercially available ELISA kit (R&D Systems, Minneapolis, MN) as per the kit protocol. The intra-assay and interassay coefficients of variation were 2.8% and 4.0%, respectively. Blood urea nitrogen was analyzed using a commercially available colorimetric urea assay (Arbor Assays, Ann Arbor, MI) as per the kit protocol. The intra-assay and interassay coefficients of variation were 4.5% and 3.9%, respectively. Plasma cystatin C was determined using a commercially available ELISA from R&D Systems. The intra-assay and interassay coefficients of variation were 3.8% and 8.3%, respectively.

Kidney and ileum histology. Kidneys were fixed in 10% (vol/vol) neutral buffered formalin before being embedded in paraffin. Kidney sections (3 μm) were stained with periodic acid-Schiff and assessed in a semiquantitative manner, whereby a blinded researcher assessed the level of glomerulosclerosis for each glomerulus and assigned an integer score between 1 and 4, indicative of the level of severity of glomerulosclerosis. Twenty-five glomeruli were scored per animal, and these scores were averaged to provide a glomerulosclerosis score index for each animal, as previously described (6). Ileal sections were fixed in 4% paraformaldehyde for 24 h followed by a transfer to 4% sucrose and subsequent embedding in paraffin. Ileal sections (5 μm) were stained with hematoxylin and eosin, and images were captured using a bright-field microscope (Nikon Eclipse-Ci, Nikon, Tokyo, Japan) coupled with a digital camera (Nikon DS-Fi3, Nikon). Morphological measurements of villus height and crypt depth were conducted using ImageJ (version 1.52a). Villus height was measured from the topmost point of the villus to the crypt transition, while the crypt depth was measured as the invagination between two villi to the basement membrane.

Quantitative RT-PCR. RNA was isolated from the snap-frozen renal cortex and ileum using a phenol-chloroform extraction method and used to synthesize cDNA as previously described (6). Gene expression of claudin-1 (*Cldn1*), claudin-3 (*Cldn3*), occludin (*Ocln*), and GPR109a (*Hcar2*) were determined using SYBR green reagents (Applied Biosystems), while expression of zonula occludens (*Tjp1*) and junction adhesion molecule 1 (JAM-1; *F11r*) were determined using TaqMan (Life Technologies, Carlsbad, CA). Gene expression was normalized to 18S rRNA using the $\Delta\Delta C_t$ method (where C_t is threshold cycle) and reported as fold change compared with WT nondiabetic mice that received the control diet.

Statistical analyses. Data were analyzed by two-way ANOVA with Tukey's post hoc test for multiple comparisons. Analyses were performed using GraphPad Prism (version 7.01, GraphPad Software, La Jolla, CA). Data are shown as means ± SE. P values of <0.05 were considered statistically significant.

RESULTS

Metabolic and phenotypic parameters. Consistent with the diabetic phenotype, mice with STZ-induced diabetes had increased glycated hemoglobin and decreased body weight (Table 1). Diabetes was associated with a decrease in relative fat mass and an increased lean mass and increased 24-h urine output and water intake (Table 1). Neither deletion of GPR109a nor consumption of the high-fiber (RS) diet was associated with changes in GHb, body weight, or body composition. Diabetes was associated with an increased liver

Table 1. *Phenotypic and biochemical characteristics of mice*

	Nondiabetic				Diabetic						
	WT CON	WT HF	KO CON	KO HF	Diab WT CON	Diab WT HF	Diab KO CON	Diab CON HF	Interaction	Genotype/ Diet	Diab
Body weight, g	35.6 ± 1.2	34.9 ± 1.6	37.7 ± 2.1	35.6 ± 1.4	24.3 ± 0.8	21.9 ± 0.6	22.3 ± 1.2	24.9 ± 1.0	NS	NS	‡
Glycated hemoglobin, %	4.0 ± 0.0	4.3 ± 0.2	4.1 ± 0.1	4.0 ± 0.1	11.9 ± 0.5	12.3 ± 0.3	11.6 ± 0.5	11.8 ± 0.5	NS	NS	‡
Fat mass, %	19.4 ± 1.7	19.5 ± 2.5	22.0 ± 1.7	20.7 ± 2.1	2.1 ± 0.5	1.4 ± 0.5	1.1 ± 0.5	1.0 ± 1.0	NS	NS	‡
Lean mass, %	77.1 ± 1.6	77.0 ± 2.3	74.5 ± 1.7	75.8 ± 2.1	90.1 ± 0.5	90 ± 0.6	87.5 ± 0.7	89.7 ± 0.6	NS	NS	‡
Urine output	1.8 ± 0.2	2.0 ± 0.2	1.7 ± 0.1	1.8 ± 0.2	5.3 ± 0.3	5.6 ± 0.2	5.1 ± 0.3	4.8 ± 0.4	NS	NS	‡
Water intake	0.7 ± 0.1	1.0 ± 0.1	0.9 ± 0.1	1.0 ± 0.1	19.6 ± 2.2	18.7 ± 1.0	17.7 ± 2.0	16.4 ± 2.6	NS	NS	‡
Liver, %	3.9 ± 0.2	4.3 ± 0.2	4.4 ± 0.2	4.2 ± 0.2	5.4 ± 0.2	5.5 ± 0.2	6.0 ± 0.4	6.0 ± 0.4	NS	NS	‡
Spleen, %	0.3 ± 0.0	0.3 ± 0.0*	0.3 ± 0.0	0.4 ± 0.1*	0.3 ± 0.0	0.2 ± 0.0	0.3 ± 0.0	0.3 ± 0.0	NS	NS	†

Data are expressed as means ± SE; n = 7–14. Fat mass, lean mass, liver weight, and spleen weight are expressed as % g/g body wt. WT, wild type; CON, control diet; HF, high-fiber diet; KO, knockout; Diab, diabetes; NS, not significant. Two-way ANOVA followed by Tukey's multiple-comparisons test was used to evaluate results. *For the post hoc test, cells within rows sharing the same superscript are significantly different from each other ($P < 0.05$). †$P < 0.05$; ‡$P < 0.0001$.

weight and a decreased spleen weight (Table 1). Mice with diabetes had an increase in small intestine length ($P < 0.001$; Fig. 1*A*), cecum length ($P < 0.0001$; Fig. 1*B*), small intestine weight ($P < 0.0001$; Fig. 1*D*), cecum weight ($P < 0.0001$; Fig. 1*E*), and colon weight ($P < 0.0001$; Fig. 1*F*). Consumption of the fiber supplement led to an increase in cecal weight and length in diabetic mice but not in nondiabetic mice (Fig. 1, *B* and *E*). RS supplementation was also associated with an increase in colon weight (Fig. 1*F*).

Renal injury and inflammation. Diabetic mice exhibited the hallmarks of diabetic nephropathy, including albuminuria ($P < 0.0001$; Fig. 2*A*), increased blood urea nitrogen ($P < 0.0001$; Fig. 2*B*), renal hypertrophy ($P < 0.0001$; Fig. 2*C*), and hyperfiltration ($P < 0.0001$; Fig. 2*D*). Genetic ablation of *Gpr109a* resulted in no change in the renal phenotype in diabetic mice (Fig. 2, *A–D*). Likewise, the high-fiber diet in the context of diabetes did not alter hallmarks of diabetic nephropathy (Fig. 2, *A–D*). Diabetes was associated with an increase in the inflammatory marker MCP-1, while there was no effect of either RS supplementation or deletion of *Gpr109a* ($P < 0.0001$; Fig. 2*E*). The state of diabetes was associated with an increase in the renal expression of GPR109a (*Hcar2*), which was mitigated with RS supplementation ($P < 0.05$; Fig. 2*F*). Assessment of renal histology revealed an overall increase in glomerulosclerosis in the diabetic setting; however, genetic ablation of *GPR109a* or supplementation with the high-fiber diet did not impact on renal structural injury ($P < 0.0001$; Fig. 3, *A* and *B*).

Intestinal permeability and morphology. To determine whether *Gpr109a* deletion led to changes in intestinal morphology, histology of the ileum was undertaken. Diabetes was associated with an overall increase in villi height ($P < 0.0001$; Fig. 4, *A* and *C*) and a reduction in crypt depth ($P < 0.001$; Fig. 4, *B* and *C*) in the ileum. In nondiabetic mice, deletion of *GPR109a* was associated with a trend toward increased villi height ($P = 0.06$; Fig. 4*A*). The high-fiber diet led to a trend toward an increase in villi height in nondiabetic WT and *Gpr109a*$^{-/-}$ diabetic mice (Fig. 4*A*). Despite these morphological changes in the ileum with diabetes, diabetes did not induce any alteration in intestinal permeability, as measured by an in vivo intestinal permeability procedure (dextran-FITC; Fig. 4*D*) or as determined by gene expression of the tight junction proteins occludin (*Ocln*; Fig. 4*E*), zonula occludens (*Tjp1*; Fig. 4*F*), JAM-1 (*F11r*; Fig. 4*G*), claudin-1 (*Cldn-1*; Fig. 4*H*), or claudin-3 (*Cldn-3*; Fig. 4*I*).

DISCUSSION

The present study explored the effects that genetic deletion of the butyrate receptor, GPR109a, had on the development of chronic renal injury in diabetic nephropathy. No effect on the diabetic renal phenotype was observed with deletion of *Gpr109a*. Surprisingly, there was no change in intestinal permeability or morphometry as a result of *Gpr109a* deletion. Furthermore, a high-fiber diet with 12.5% RS was not effective in reducing renal injury in the setting of diabetes.

This is the first study to assess the effects of deletion of GPR109a on diabetic nephropathy, and these findings show that deletion of this receptor was not associated with any change in renal injury in long-term experiments (24 wk). Given the hypothesis that renal injury would occur downstream of alterations in intestinal permeability, and there was no effect of *Gpr109a* deletion on in vivo assessment of intestinal permeability, this should perhaps not come as a surprise finding. In vitro, *Gpr109a* knockdown inhibits butyrate-induced increases in the tight junction protein claudin-3, suggesting that GPR109a may have a role in the integrity of the intestinal epithelial barrier (9). However, in vivo, while deletion of GPR109a was associated with a trend toward an increase in intestinal permeability in an induced food allergy model (20), there was no effect in otherwise healthy mice (5), indicating that deletion of GPR109a alone is insufficient to alter intestinal permeability. There is redundancy in the metabolite-sensing GPR family, with butyrate being recognized by GPR109a, GPR41, and GPR43. Indeed, it has been suggested that given this redundancy, single knockout models are insufficient to fully elucidate the effects of these receptors and that double or triple knockout models are required (21).

RS is a type of dietary fiber that acts as a prebiotic. Numerous studies have illustrated that supplementation with RS is associated with an increase in the microbial production of SCFAs, particularly butyrate (19). A commonly used source of RS is HAMS, and in an obese model of diabetes, the Zucker diabetic fatty rat, 6 wk of supplementation with a diet containing 55% HAMS (Amylogel, equivalent to 20% RS) was associated with a reduction in albuminuria (13). In addition, in the adenine-induced rat model of chronic kidney disease, supplementation with 59% HAMS diet (Hi-maize 260, equivalent to 27% RS) for 3 wk was associated with improvements in creatinine clearance (22). Conversely, however, a study that

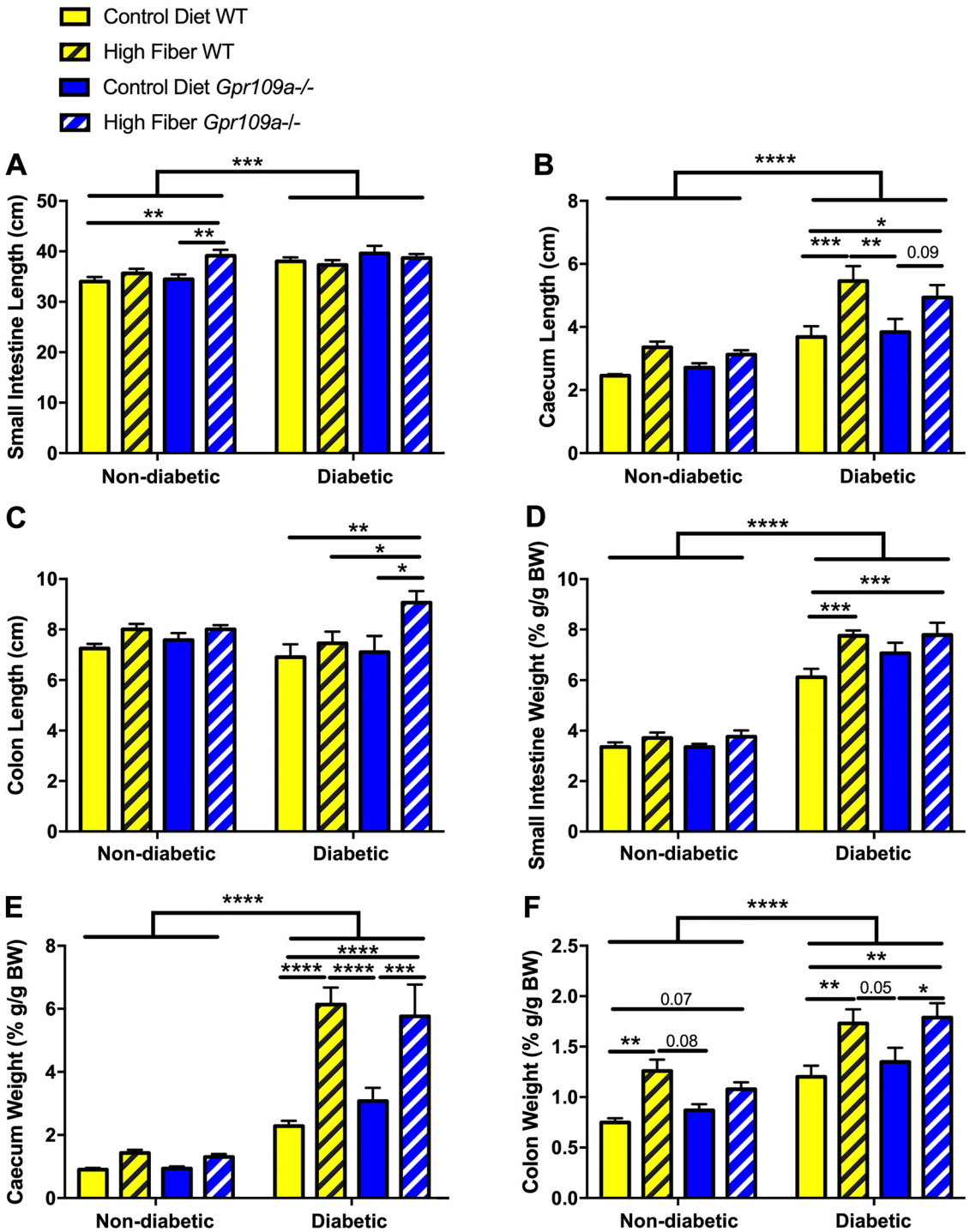

Fig. 1. Intestinal anatomy. *A*: small intestine length. *B*: cecum length. *C*: colon length. *D*: small intestine weight. *E*: cecum weight. *F*: colon weight. WT, wild type; GPR109a, G protein-coupled receptor 109a. Data are expressed as means ± SE; $n = 7$–12. *$P < 0.05$; **$P < 0.01$; ***$P < 0.001$; ****$P < 0.0001$.

supplemented a diet containing 55% HAMS (Amylogel, equivalent to 20% RS) for 4 wk in male Sprague-Dawley rats with STZ-induced diabetes did not find any renoprotective benefit with RS supplementation (12). Although these results show promise, the concentrations of HAMS used in these studies are likely to be much greater than could be reasonably expected to be consumed by people.

Since previous studies exploring the role of RS on the development of renal injury have used supraphysiological doses over a short period of time, we sought to supplement a dose of RS that could be more reasonably expected to be consumed by people (25% HAMS Hi-maize 1043, equivalent to 12.5% RS) over a longer timeframe (24 wk). In the present study, we investigated the effects of RS supplementation, at a dose of ~12.5%, on the development of diabetic nephropathy in the STZ-induced diabetic mouse. Supplementation of a high-fiber RS diet in such chronic studies was not renoprotective.

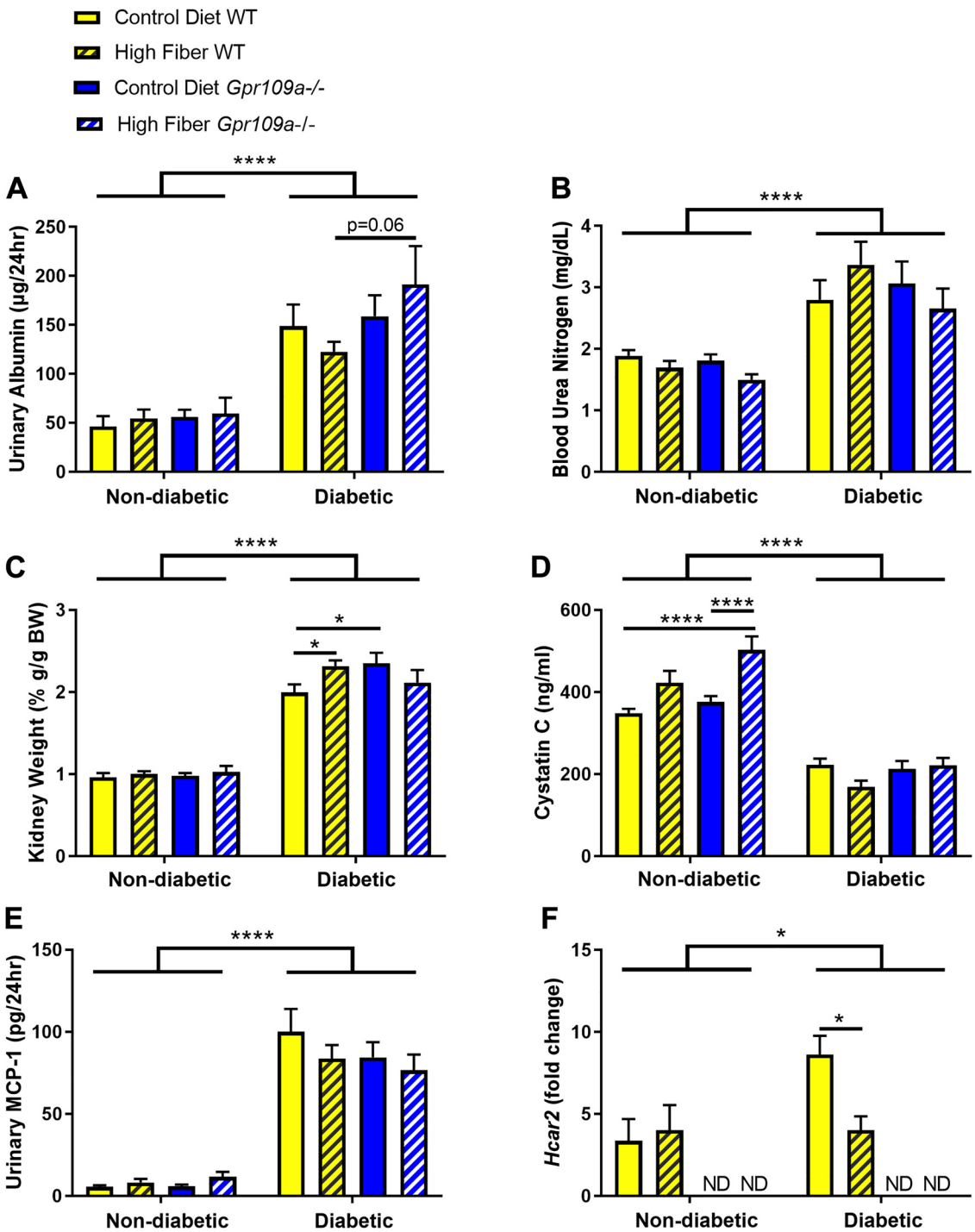

Fig. 2. Renal injury and inflammation. *A*: urine albumin. *B*: blood urea nitrogen. *C*: relative kidney weight. *D*: plasma cystatin C. *E*: urinary monocyte chemoattractant protein-1 (MCP-1). *F*: kidney expression of G protein-coupled receptor 109a (GPR109a; *Hcar2*). WT, wild type; BW, body weight; ND, not determined. Data are expressed as means ± SE; $n = 7$–14. *$P < 0.05$; ****$P < 0.0001$.

A recent study (8) has shown a renoprotective effect of butyrate on adriamycin-induced nephropathy in short-term experiments. In that study, intraperitoneal injection of butyrate for 7 or 14 days in a model of adriamycin-induced nephropathy and dietary supplementation of a high-fiber butyrylated RS diet for 4 wk before adriamycin-induced nephropathy (preventative approach) showed that butyrate led to a decreased urinary protein-to-creatinine ratio. Although no measures of intestinal permeability were determined, that study shows promise for butyrate as a renoprotective agent, at least in the acute setting, most likely attributable to acute inflammation.

A limitation of the present study is the animal model of diabetic nephropathy that was used. Chemical induction of diabetes, such as with STZ, is useful as it can be applied regardless of genetic background for assessing the effects of diabetes. However, concerns have been raised that the STZ-

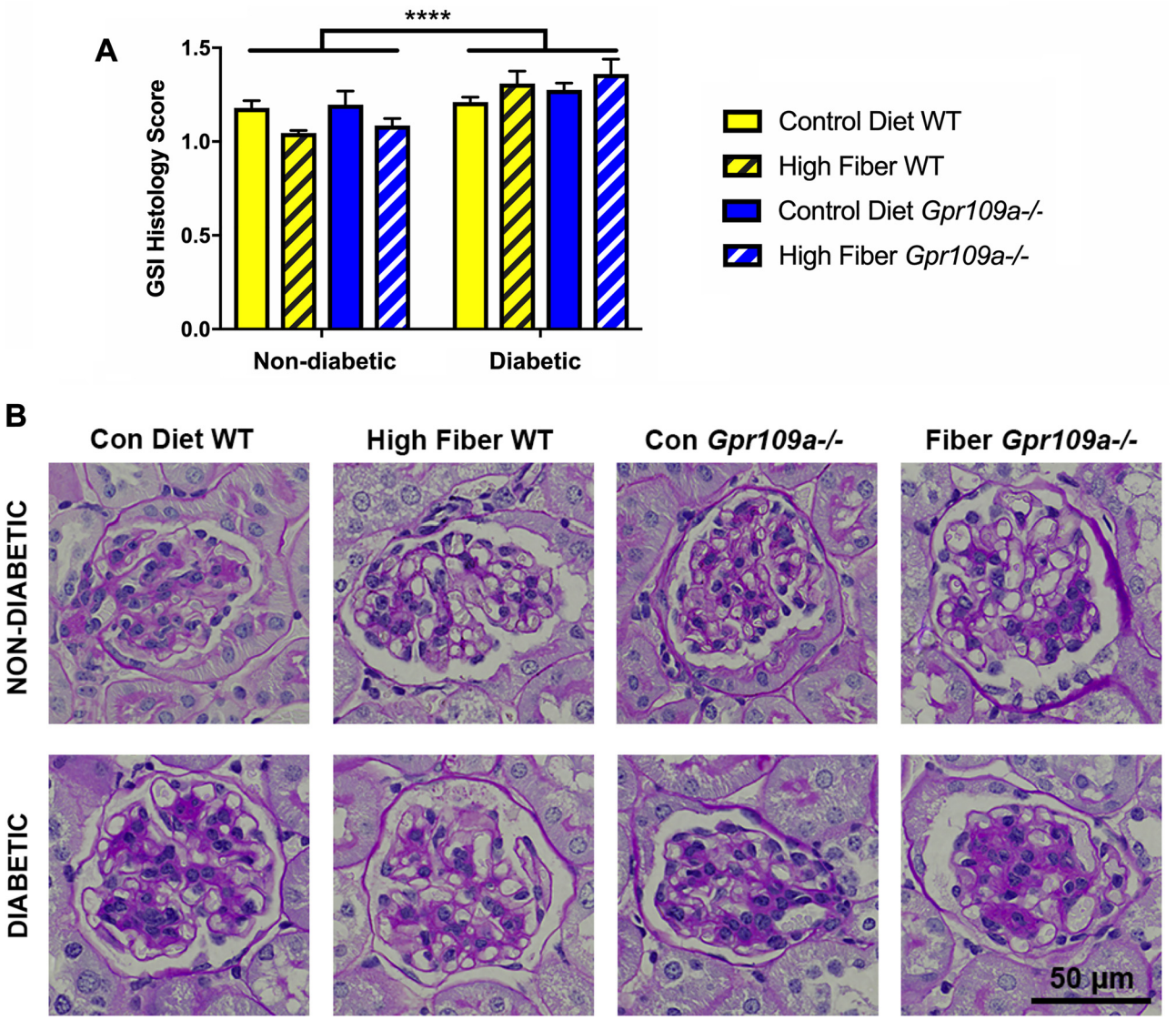

Fig. 3. Renal structural changes. *A*: glomerulosclerotic index score (GSI). *B*: representative periodic acid-Schiff-stained images. WT, wild type; GPR109a, G protein-coupled receptor 109a; Con, control Data are expressed as means ± SE; $n = 7–12$. ****$P < 0.0001$.

induced mouse model does not adequately recapitulate the features of human diabetic nephropathy (2, 3). Furthermore, the *Gpr109a*$^{-/-}$ mice used in the present study were on a C57/BL6 background. Mice bred on this background are known to develop less renal injury when exposed to STZ compared with mice on the DBA/2J or FVB/NJ backgrounds (18). The Animal Models of Diabetic Complications Consortium has suggested that the Ins2 Akita mouse, featuring a genetic mutation in the Ins2 protein, is a preferable model for assessment of diabetic nephropathy in type 1 diabetes mellitus (2). Future research in this area may benefit from cross-breeding genetic deletion models, such as the *Gpr109a*$^{-/-}$ mouse used in the present study, with genetic models of diabetes, such as the Ins2 Akita mouse.

In conclusion, this study shows that long-term RS supplementation, at a dosage that would reasonably be expected to be consumed by humans, did not alleviate albuminuria in the STZ-induced diabetes model. While diabetes was associated with alterations in intestinal morphology, there was no change in intestinal permeability. It would be pertinent to consider RS supplementation in other rodent models of diabetes that may be more representative of the intestinal changes that occur with diabetes in humans. Finally, this study indicates that GPR109a deletion does not play a critical role in the development of diabetic nephropathy or gastrointestinal homeostasis.

ACKNOWLEDGMENTS

The authors thank the following people: Maryann Arnstein for technical assistance, Prof. Charles R. Mackay (Monash University) for the *Gpr109a*$^{-/-}$ mice, and Warren Potts from Specialty Feeds for the design and generation of the diets.

GRANTS

M. Snelson and R. S. J. Lindblom were supported by scholarships from the Australian government Research Training Program. G. C. Higgins was supported by a postdoctoral fellowship from the Juvenile Diabetes Research Foundation (JDRF). S. M. Tan is supported by a JDRF Advanced Postdoctoral Fellowship, and M. T. Coughlan is supported by a Career Development Award from the JDRF Type 1 Diabetes Clinical Research Network, a special research initiative of the Australian Research Council.

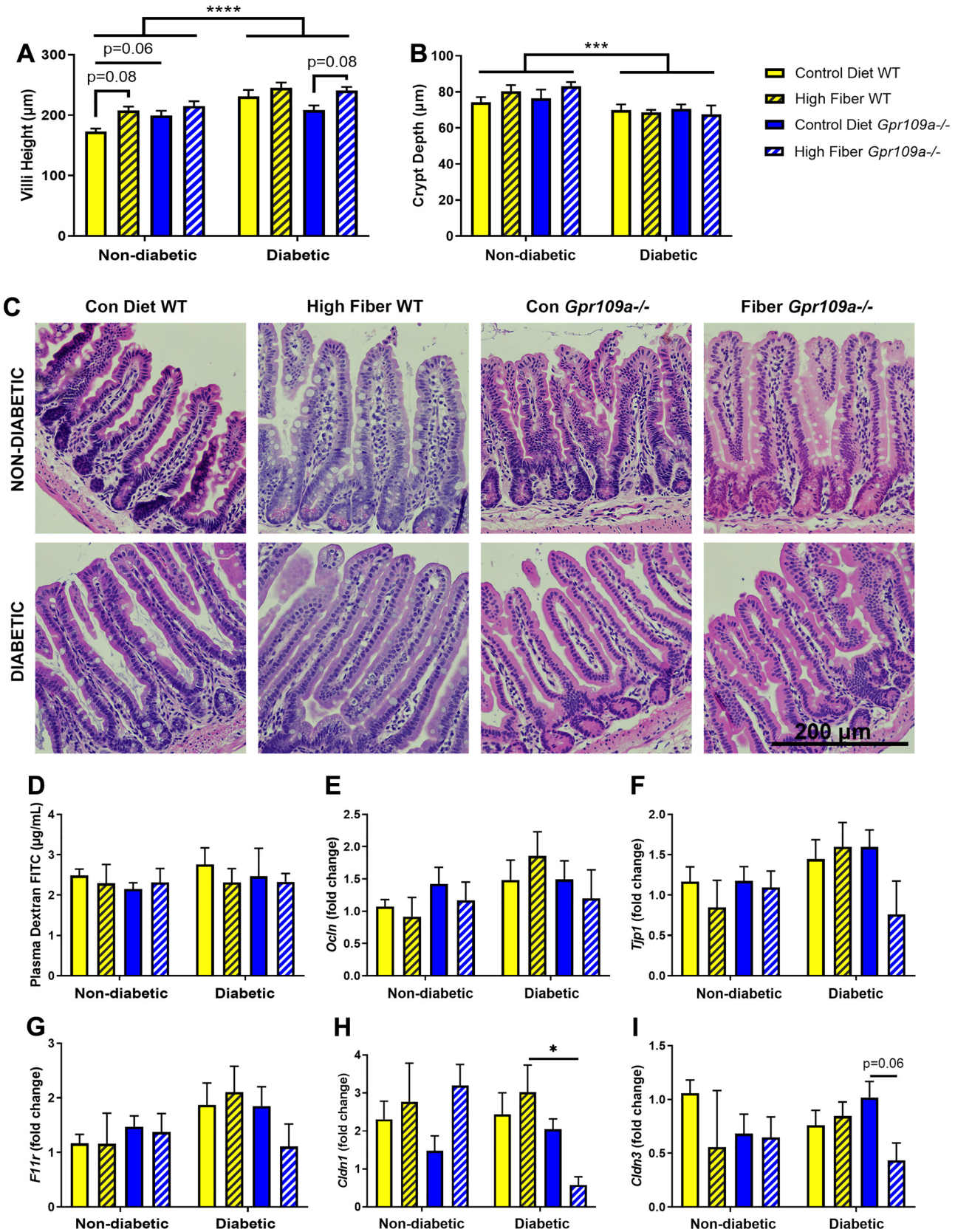

Fig. 4. Intestinal permeability and morphology. *A*: ileum villi height. *B*: ileum crypt depth. *C*: representative hematoxylin and eosin-stained images. *D*: plasma dextran-FITC intestinal permeability assay. *E*: ileum expression of occludin (*Ocln*). *F*: ileum expression of zonula occludens (*Tjp1*). *G*: ileum expression of junction adhesion molecule 1 (*F11r*). *H*: ileum expression of claudin 1 (*Cldn1*). *I*: ileum expression of claudin 3 (*Cldn3*). WT, wild type; GPR109a, G protein-coupled receptor 109a; Con, control. Data are expressed as means ± SE; $n = 7$–12. *$P < 0.05$; ***$P < 0.001$; ****$P < 0.0001$.

DISCLOSURES

No conflicts of interest, financial or otherwise, are declared by the authors.

AUTHOR CONTRIBUTIONS

M.S. and M.T.C. conceived and designed research; M.S., S.M.T., G.C.H., and R.S.J.L. performed experiments; M.S. and M.T.C. analyzed data; M.S., S.M.T., and M.T.C. interpreted results of experiments; M.S. and M.T.C. prepared figures; M.S. and M.T.C. drafted manuscript; M.S. and M.T.C. edited and revised manuscript; M.S. and M.T.C. approved final version of manuscript.

REFERENCES

1. **Alicic RZ, Rooney MT, Tuttle KR.** Diabetic kidney disease: challenges, progress, and possibilities. *Clin J Am Soc Nephrol* 12: 2032–2045, 2017. doi:10.2215/CJN.11491116.
2. **Azushima K, Gurley SB, Coffman TM.** Modelling diabetic nephropathy in mice. *Nat Rev Nephrol* 14: 48–56, 2018. doi:10.1038/nrneph.2017.142.
3. **Brosius FC III, Alpers CE, Bottinger EP, Breyer MD, Coffman TM, Gurley SB, Harris RC, Kakoki M, Kretzler M, Leiter EH, Levi M, McIndoe RA, Sharma K, Smithies O, Susztak K, Takahashi N, Takahashi T; Animal Models of Diabetic Complications Consortium.** Mouse models of diabetic nephropathy. *J Am Soc Nephrol* 20: 2503–2512, 2009. doi:10.1681/ASN.2009070721.
4. **Cani PD, Possemiers S, Van de Wiele T, Guiot Y, Everard A, Rottier O, Geurts L, Naslain D, Neyrinck A, Lambert DM, Muccioli GG, Delzenne NM.** Changes in gut microbiota control inflammation in obese mice through a mechanism involving GLP-2-driven improvement of gut permeability. *Gut* 58: 1091–1103, 2009. doi:10.1136/gut.2008.165886.
5. **Chen G, Ran X, Li B, Li Y, He D, Huang B, Fu S, Liu J, Wang W.** Sodium butyrate inhibits inflammation and maintains epithelium barrier integrity in a TNBS-induced inflammatory bowel disease mice model. *EBioMedicine* 30: 317–325, 2018. doi:10.1016/j.ebiom.2018.03.030.
6. **Coughlan MT, Higgins GC, Nguyen TV, Penfold SA, Thallas-Bonke V, Tan SM, Ramm G, Van Bergen NJ, Henstridge DC, Sourris KC, Harcourt BE, Trounce IA, Robb PM, Laskowski A, McGee SL, Genders AJ, Walder K, Drew BG, Gregorevic P, Qian H, Thomas MC, Jerums G, Macisaac RJ, Skene A, Power DA, Ekinci EI, Wijeyeratne XW, Gallo LA, Herman-Edelstein M, Ryan MT, Cooper ME, Thorburn DR, Forbes JM.** Deficiency in apoptosis-inducing factor recapitulates chronic kidney disease via aberrant mitochondrial homeostasis. *Diabetes* 65: 1085–1098, 2016. doi:10.2337/db15-0864.
7. **Evenepoel P, Poesen R, Meijers B.** The gut-kidney axis. *Pediatr Nephrol* 32: 2005–2014, 2017. doi:10.1007/s00467-016-3527-x.
8. **Felizardo RJF, de Almeida DC, Pereira RL, Watanabe IKM, Doimo NTS, Ribeiro WR, Cenedeze MA, Hiyane MI, Amano MT, Braga TT, Ferreira CM, Parmigiani RB, Andrade-Oliveira V, Volpini RA, Vinolo MAR, Mariño E, Robert R, Mackay CR, Camara NOS.** Gut microbial metabolite butyrate protects against proteinuric kidney disease through epigenetic- and GPR109a-mediated mechanisms. *FASEB J* 33: 11,894–11,908, 2019. doi:10.1096/fj.201901080R.
9. **Feng W, Wu Y, Chen G, Fu S, Li B, Huang B, Wang D, Wang W, Liu J.** Sodium butyrate attenuates diarrhea in weaned piglets and promotes tight junction protein expression in colon in a GPR109A-dependent manner. *Cell Physiol Biochem* 47: 1617–1629, 2018. doi:10.1159/000490981.
10. **Forslund K, Hildebrand F, Nielsen T, Falony G, Le Chatelier E, Sunagawa S, Prifti E, Vieira-Silva S, Gudmundsdottir V, Pedersen HK, Arumugam M, Kristiansen K, Voigt AY, Vestergaard H, Hercog R, Costea PI, Kultima JR, Li J, Jørgensen T, Levenez F, Dore J, Nielsen HB, Brunak S, Raes J, Hansen T, Wang J, Ehrlich SD, Bork P, Pedersen O.** Disentangling type 2 diabetes and metformin treatment signatures in the human gut microbiota. *Nature* 528: 262–266, 2015. [Erratum in Nature 545: 116, 2017] doi:10.1038/nature15766.
11. **Jiang S, Xie S, Lv D, Wang P, He H, Zhang T, Zhou Y, Lin Q, Zhou H, Jiang J, Nie J, Hou F, Chen Y.** Alteration of the gut microbiota in Chinese population with chronic kidney disease. *Sci Rep* 7: 2870, 2017. doi:10.1038/s41598-017-02989-2.
12. **Koh GY, Rowling MJ, Schalinske KL, Grapentine K, Loo YT.** Consumption of dietary resistant starch partially corrected the growth pattern despite hyperglycemia and compromised kidney function in streptozotocin-induced diabetic rats. *J Agric Food Chem* 64: 7540–7545, 2016. doi:10.1021/acs.jafc.6b03808.
13. **Koh GY, Whitley EM, Mancosky K, Loo YT, Grapentine K, Bowers E, Schalinske KL, Rowling MJ.** Dietary resistant starch prevents urinary excretion of vitamin D metabolites and maintains circulating 25-hydroxycholecalciferol concentrations in Zucker diabetic fatty rats. *J Nutr* 144: 1667–1673, 2014. doi:10.3945/jn.114.198200.
14. **Lancaster GI, Henstridge DC.** Body composition and metabolic caging analysis in high-fat fed mice. *J Vis Exp* 57280, 2018. doi:10.3791/57280.
15. **Le Leu RK, Hu Y, Brown IL, Young GP.** Effect of high amylose maize starches on colonic fermentation and apoptotic response to DNA-damage in the colon of rats. *Nutr Metab (Lond)* 6: 11, 2009. doi:10.1186/1743-7075-6-11.
16. **Macia L, Tan J, Vieira AT, Leach K, Stanley D, Luong S, Maruya M, Ian McKenzie C, Hijikata A, Wong C, Binge L, Thorburn AN, Chevalier N, Ang C, Marino E, Robert R, Offermanns S, Teixeira MM, Moore RJ, Flavell RA, Fagarasan S, Mackay CR.** Metabolite-sensing receptors GPR43 and GPR109A facilitate dietary fibre-induced gut homeostasis through regulation of the inflammasome. *Nat Commun* 6: 6734, 2015. doi:10.1038/ncomms7734.
17. **Meijers B, Farré R, Dejongh S, Vicario M, Evenepoel P.** Intestinal barrier function in chronic kidney disease. *Toxins (Basel)* 10: 298, 2018. doi:10.3390/toxins10070298.
18. **Qi Z, Fujita H, Jin J, Davis LS, Wang Y, Fogo AB, Breyer MD.** Characterization of susceptibility of inbred mouse strains to diabetic nephropathy. *Diabetes* 54: 2628–2637, 2005. doi:10.2337/diabetes.54.9.2628.
19. **Snelson M, Kellow NJ, Coughlan MT.** Modulation of the gut microbiota by resistant starch as a treatment of chronic kidney diseases: evidence of efficacy and mechanistic insights. *Adv Nutr* 10: 303–320, 2019. doi:10.1093/advances/nmy068.
20. **Tan J, McKenzie C, Vuillermin PJ, Goverse G, Vinuesa CG, Mebius RE, Macia L, Mackay CR.** Dietary fiber and bacterial SCFA enhance oral tolerance and protect against food allergy through diverse cellular pathways. *Cell Reports* 15: 2809–2824, 2016. doi:10.1016/j.celrep.2016.05.047.
21. **Tan JK, McKenzie C, Mariño E, Macia L, Mackay CR.** Metabolite-sensing G protein-coupled receptors-facilitators of diet-related immune regulation. *Annu Rev Immunol* 35: 371–402, 2017. doi:10.1146/annurev-immunol-051116-052235.
22. **Vaziri ND, Liu S-M, Lau WL, Khazaeli M, Nazertehrani S, Farzaneh SH, Kieffer DA, Adams SH, Martin RJ.** High amylose-resistant starch diet ameliorates oxidative stress, inflammation, and progression of chronic kidney disease. *PLoS One* 9: e114881, 2014. doi:10.1371/journal.pone.0114881.
23. **Wong J, Piceno YM, DeSantis TZ, Pahl M, Andersen GL, Vaziri ND.** Expansion of urease- and uricase-containing, indole- and p-cresol-forming and contraction of short-chain fatty acid-producing intestinal microbiota in ESRD. *Am J Nephrol* 39: 230–237, 2014. doi:10.1159/000360010.